NOTES AND CORRESPONDENCE

Influence of Geostrophic Wind on Atmospheric Nocturnal Cooling

CLAUDE ESTOURNEL AND DANIEL GUEDALIA

Laboratoire d'Aérologie, 31062 Toulouse Cedex, France

28 February 1985 and 21 June 1985

ABSTRACT

A dynamic radiative model was used to study the influence of the geostrophic wind on the nocturnal cooling processes. For weak wind conditions, an important difference appears between the top levels of the inversion and turbulent layers. The dimensionless vertical profile of turbulent heat flux presents an important curvature at the beginning of the night; afterwards this profile varies little during the night.

1. Introduction

In the past few years other authors have studied the contribution of radiative cooling to the evolution of the nocturnal boundary layer (NBL). Coantic and Seguin (1971) analytically studied how the radiative term affects the surface layer structure. Later, several numerical models were developed that considered both radiative and turbulent transfer (André *et al.*, 1978; Yamada, 1979; Nieuwstadt, 1984). More recently, Garratt and Brost (1981) performed a set of simulations to display the influence of radiation on the vertical structure of the NBL; these simulations were only run for one value of the geostrophic wind (10 m s^{-1}). André and Mahrt (1982) studied the contribution of the radiative and turbulent cooling through 17 nights of the Wangara and Voves experiments. They deduced that the turbulent cooling is located in the low part of the NBL and that the radiative cooling allows the development of the inversion layer; however, the heat budget (turbulent and radiative) varies significantly between individual cases. Because of the experimental difficulties to obtain values of turbulent and radiative fluxes under varied situations, it seems necessary to use numerical simulations to investigate the parameters that influence the contribution of turbulence and radiation to the nocturnal cooling.

For a clear night, the three parameters that determine the evolution of the NBL structure are the geostrophic wind speed, the surface roughness and the ground cooling rate. Delage (1974) showed that a tenfold increase in surface roughness leads to an increase of less than 10% in the inversion height. Thus, for fixed soil characteristics, the most important parameter driving the NBL evolution is the geostrophic wind. The purpose of this paper is to show precisely that the contribution of radiative and turbulent terms to the evolution of the NBL is strongly dependent of the geostrophic wind speed.

2. Nocturnal boundary layer model

We used a one-dimensional model to compute the time evolution of wind and temperature from the following equations:

$$\frac{\partial \theta}{\partial t} = \frac{\partial}{\partial z} K \frac{\partial \theta}{\partial z} - R_r \tag{1}$$

$$\frac{\partial u}{\partial t} = \frac{\partial}{\partial z} K \frac{\partial u}{\partial z} + f \cdot (v - v_g) \tag{2}$$

$$\frac{\partial v}{\partial t} = \frac{\partial}{\partial z} K \frac{\partial v}{\partial z} - f \cdot (u - u_g) \tag{3}$$

$$\frac{\partial T_s}{\partial z} = \frac{\partial}{\partial z} K_s \frac{\partial T_s}{\partial z}, \tag{4}$$

where θ is the potential temperature; u and v are the mean wind components; subscript g refers to the geostrophic wind; K is the eddy exchange coefficient; T_s and K_s are the soil temperature and exchange coefficient; R_r is the radiative cooling rate; and f is the Coriolis parameter.

The major points of this model are:

1) the heat and momentum turbulent fluxes are expressed with the use of eddy exchange coefficients computed from the turbulent kinetic energy equation (Delage, 1974);
2) the radiative cooling rate is computed with a high spectral resolution model described in Estournel *et al.* (1983) and Guedalia *et al.* (1984); and
3) the surface temperature is calculated from the surface energy balance.

The equations were solved by an implicit finite difference scheme at 50 levels between the surface and 1500 m, and 5 levels between the surface and 1 m below the surface.

Initial conditions are given by the steady state solution for the neutrally stratified boundary layer. The lower boundary condition (level -1 m) is the time-constant temperature. At the top of the model, heat and momentum fluxes are set to 0. The simulations presented here were performed with a soil thermal conductivity of 0.75 W m^{-1} K^{-1} and a soil exchange coefficient of 4.7×10^{-7} m^2 s^{-1} corresponding to moist soil. A value of 1.1×10^{-4} s^{-1} was chosen for the Coriolis parameter (midlatitude).

3. Cooling rate

Two simulations are presented here with all parameters identical except the geostrophic wind which allows variation of the turbulence intensity. Two values were chosen: $G = 10$ m s^{-1} (run A10) and $G = 3$ m s^{-1} (run A3). Figure 1 shows the evolution of the nocturnal potential temperature profile for both cases. The values of h_i (inversion height) and h_t (turbulent layer height) are also indicated; h_i is defined according to André and Mahrt (1982) as the height where the potential temperature gradient is equal to 3.5×10^{-3} K m^{-1}, and h_t is defined as the altitude where the heat flux is 5% of its surface value.

Figure 2 shows the vertical profiles of the radiative and turbulent cooling rate computed at different times after the beginning of the night.

For strong wind conditions (run A10), turbulent cooling prevails in the inversion layer while for run A3, turbulent and radiative cooling are of the same order; for weak wind conditions (run A3), radiative cooling presents a strong vertical gradient that acts to stabilize the atmosphere above the turbulent layer; it can be seen in Fig. 1 that h_t has little variation all night long while h_i increases in an important way. On the other hand, for strong wind conditions (run A10), radiative cooling varies little with altitude and thus the depth of the stable layer overlying the turbulent layer remains nearly constant. This explains the differences between the depths of the inversion and turbulent layers observed by André and Mahrt (1982) from experimental data.

One may observe a strong vertical gradient of turbulent cooling at the beginning of the night no matter what the wind speed; it is just this gradient that leads to the formation of the nocturnal inversion.

4. Turbulent heat flux

Figure 3 shows the vertical profiles of dimensionless heat fluxes computed at different times of the night for runs A3 and A10. The turbulent heat fluxes were non-dimensionalized by their surface value and the altitude by the turbulent layer depth h_t. It appears that the heat flux profiles present during the first hour of cooling have significant curvature that is more important under strong wind conditions. After the transition period

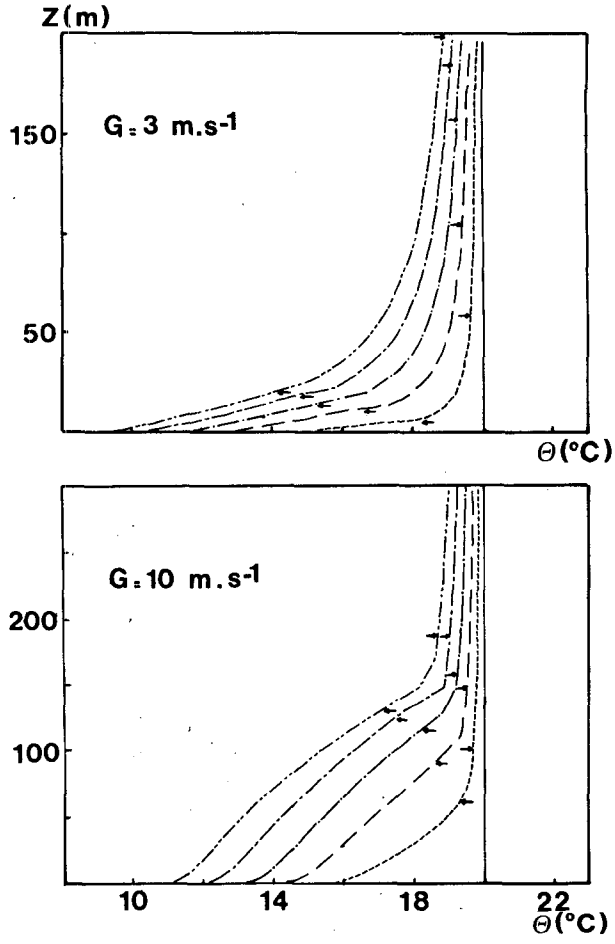

FIG. 1. Potential temperature profiles computed for two values of the geostrophic wind at different times after transition, (solid line): initial; (short-dashed line): 2 h; (long-dashed line): 4 h; (dash-dot line): 6h; (short-long dashed line): 8 h; (long–double short dashed line): 10 h. (right arrow): inversion layer height h_i; (left arrow): turbulent layer height h_t.

(here, about the first two hours of cooling), the dimensionless heat flux profile presents little variation during the night and approaches a linear shape when the wind is strong. This important difference of turbulent heat flux profiles between the beginning and the second part of the night is possibly the reason that explains the difference noted by Nieuwstadt (1984) between the Minnesota data (Caughey *et al.*, 1979) measured during the transition period and those taken during the Cabauw experiments, which avoid the first hours of the night.

5. Conclusion

The purpose of this note is to show that the nocturnal cooling processes in the atmosphere are very dependent on the turbulence conditions resulting from the mag-

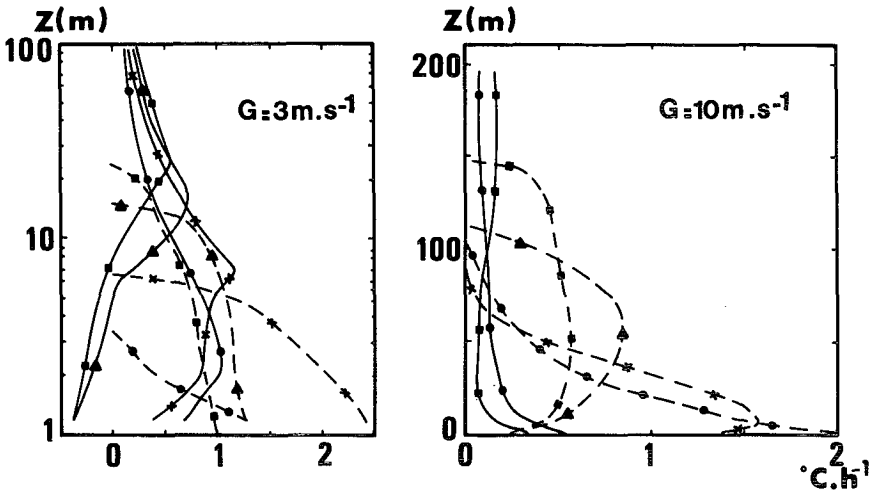

FIG. 2. Computed atmospheric cooling rate averaged on different time periods after transition. Solid line: radiative cooling rate, dashed line: turbulent cooling rate, (dots): between 0.5 and 0.75 hour; (crosses): between 1 and 2 hours; (triangles): between 3 and 4 hours; (squares): between 6 and 7 hours.

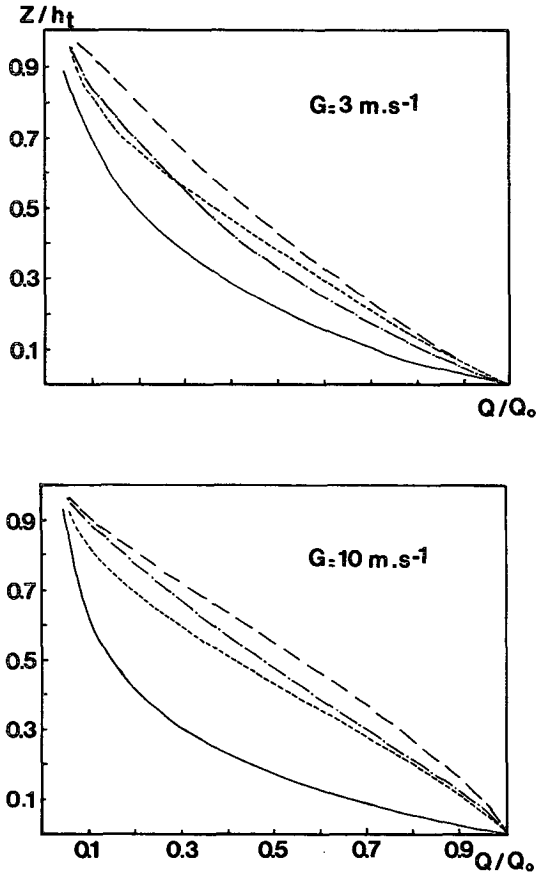

FIG. 3. Computed dimensionless turbulent heat flux at different times after transition. (solid line): 1 h; (short-dashed line): 2 h; (long-dashed line): 4 h; (dot-dashed line): 8 h.

nitude of the geostrophic wind. The simulations presented here explain that for weak wind cases, the stable layer thickens all night long because of the strong vertical gradient of radiative cooling; then, an important difference between the top of the inversion layer and the depth of the turbulent layer appears. On the other hand, for the strong wind cases, the depth of the stable layer presents little variation during the night. It emphasizes the difficulty met by many authors to parameterize the height of the nocturnal inversion without taking account of the radiative cooling. The vertical profile of turbulent heat flux presents an important curvature at the beginning of the night (formation of the inversion layer). After that, this profile presents little variation during the night.

Finally, it appears that two different layers can be distinguished: the first one near the ground, being several tens of meters deep, where turbulence occurs and can be analyzed with local parameters, and the second one, just above the first, in which turbulence is absent, and that is cooled radiatively and then is submitted more to the influence of mesoscale circulation.

Acknowledgments. The authors wish to thank S. Prieur for his participation in the model computations.

This research is supported by the A.T.P. "Recherches Atmospheriques" of Institut National d'Astronomie et Geophysique under Grant 46.46.

REFERENCES

André, J. C., and L. Mahrt, 1982: The nocturnal surface inversion and influence of clear-air radiational cooling. *J. Atmos. Sci.*, **39**, 864–878.

——, G. De Moor, P. Lacarrère, G. Therry and R. du Vachat, 1978: Modeling the 24 hour evolution of the mean and turbulent structures of the planetary boundary layer. *J. Atmos. Sci.*, **35,** 1861–1883.

Caughey, S. J., J. C. Wyngaard and J. C. Kaimal, 1979: Turbulence in the evolving stable boundary layer. *J. Atmos. Sci.*, **6,** 1041–1052.

Coantic, M., and B. Seguin, 1971: On the interaction of turbulent and radiative transfers in the surface layer. *Bound.-Layer Meteor.*, **1,** 245–263.

Delage, Y., 1974: A numerical study of the nocturnal atmospheric boundary layer. *Quart. J. Roy. Meteor. Soc.*, **100,** 351–364.

Estournel, C., R. Vehil, D. Guedalia, J. Fontan and A. Druilhet, 1983: Observations and modeling of downward radiative fluxes (solar and infrared) in urban/rural areas. *J. Climate Appl. Meteor.*, **22,** 134–142.

Garratt, J. R., and R. A. Brost, 1981: Radiative cooling effects within and above the nocturnal boundary layer. *J. Atmos. Sci.*, **38,** 2730–2746.

Guedalia, D., C. Estournel and R. Vehil, 1984: Effects of Sahel dust layers upon nocturnal cooling of the atmosphere. *J. Climate Appl. Meteor.*, **23,** 644–650.

Nieuwstadt, F. T. M., 1984: The turbulent structure of the stable nocturnal boundary layer. *J. Atmos. Sci.*, **41,** 2202–2216.

Yamada, T., 1979: Prediction of the nocturnal surface inversion height. *J. Appl. Meteor.*, **18,** 526–531.